DOI 10.1007/s10812-015-0059-2
Journal of Applied Spectroscopy, Vol. 82, No. 1, March, 2014 (Russian Original Vol. 82, No. 1, January–February, 2015)

STRUCTURE AND VIBRATIONAL SPECTRA OF URANYL DINITRATE COMPLEXES WITH WATER AND DMSO

M. B. Shundalau,* A. A. Zazhogin, A. P. Zazhogin, A. I. Komyak, and D. S. Umreiko

UDC 539.19

Structural models were designed and spectral characteristics were computed based on DFT calculations for uranyl dinitrate complexes with H_2O and DMSO [$UO_2(NO_3)_2 \cdot 2DMSO$, $UO_2(NO_3)_2 \cdot 2H_2O \cdot 2DMSO$, $UO_2(NO_3)_2 \cdot 2H_2O \cdot 4DMSO$]. Vibrational IR and Raman spectra of $UO_2(NO_3)_2 \cdot 2DMSO$ were interpreted using models for bidentate and monodentate coordination of nitrate ions to uranyl. Several spectral signatures that characterized DMSO complexation in the second coordination sphere were identified and had analytical significance.

Keywords: *density functional theory, effective core potential, infrared spectrum, Raman spectrum, uranyl dinitrate, dimethylsulfoxide, coordination complex.*

Introduction. Compounds of hexavalent uranium [U(VI)] form numerous complexes with organic and inorganic ligands [1–3]. Because the fragments of such complexes are labile, they can play an important role in the migration of U ions in degraded surface layers of nuclear materials and nuclear wastes [4]. Theoretical investigations of complexation together with experimental measurements of the characteristics of U(VI) complexes allowed definite trends in their structures and physicochemical properties to be identified [5]. Structural models were built and vibrational spectra were interpreted earlier for complexes of tetravalent (UCl_4) and hexavalent (UO_2^{2+}) uranium with polar organic ligands in the first coordination sphere ($UCl_4 \cdot 2DMF$, $UCl_4 \cdot 2DMSO$, $UCl_4 \cdot 2HMPA$, $UO_2Cl_2 \cdot 2HMPA$) based on quantum-chemical calculations and spectroscopic measurements [6–8]. Density functional theory computations demonstrated that the complex structural models were adequate and agreed with existing experimental data.

The present work discusses the structures of uranyl dinitrate [$UO_2(NO_3)_2$] complexes with H_2O and DMSO based on quantum-chemical calculations and analyses of IR and Raman spectra.

Experimental and Calculations. IR absorption spectra of $UO_2(NO_3)_2 \cdot 2DMSO$ in mineral oil were recorded on a Bruker IFS-113 Fourier spectrometer in the range 3700–600 cm^{-1}; Raman spectra of solid $UO_2(NO_3)_2 \cdot 2DMSO$, 3300–50 cm^{-1}. Excitation used radiation from an Ar-ion laser with $\lambda = 514.5$ nm and power 200 mW.

The applied quantum-chemistry program GAMESS-US [9, 10] was used to optimize the equilibrium structures and to calculate force fields, eigen frequencies of harmonic vibrations, and intensities in IR and Raman spectra of $UO_2(NO_3)_2 \cdot 2DMSO$, $UO_2(NO_3)_2$, $UO_2(NO_3)_2 \cdot 2H_2O$, $UO_2(NO_3)_2 \cdot 2H_2O \cdot 2DMSO$, and $UO_2(NO_3)_2 \cdot 2H_2O \cdot 4DMSO$ and their fragments. The results were visualized using the MacMolPlt [11] and ORTEP [12] programs. The relativistic effective core potential (RECP) LANL2DZ was used for the U atom [13] and replaced the 78 inner electrons. A DZ-basis set that was specially developed for this RECP was used for the remaining U electrons. The other atoms were described based on the standard full-electron basis cc-pVDZ of Dunning [14]. The RECP and the corresponding basis sets were generated using the Extensible Computational Chemistry Environment Basis Set Database [15–17]. The hybrid exchange-correlated functional B3LYP was also used in all calculations [18–20].

Results and Discussion. Figure 1 shows portions of the experimental IR and Raman spectra of $UO_2(NO_3)_2 \cdot 2DMSO$ in the regions 1600–600 and 1650–50 cm^{-1}. Table 1 compares the experimental data with the calculated harmonic vibrational frequencies of the anhydrous complex of $UO_2(NO_3)_2$ with DMSO in addition to its fragments and hydrates. Weak bands in

*To whom correspondence should be addressed.

Belarusian State University, 4 Nezavisimost′ Ave., Minsk, 220030, Belarus; e-mail: shundalov@bsu.by. Translated from Zhurnal Prikladnoi Spektroskopii, Vol. 82, No. 1, pp. 29–36, January–February, 2015. Original article submitted May 16, 2014.

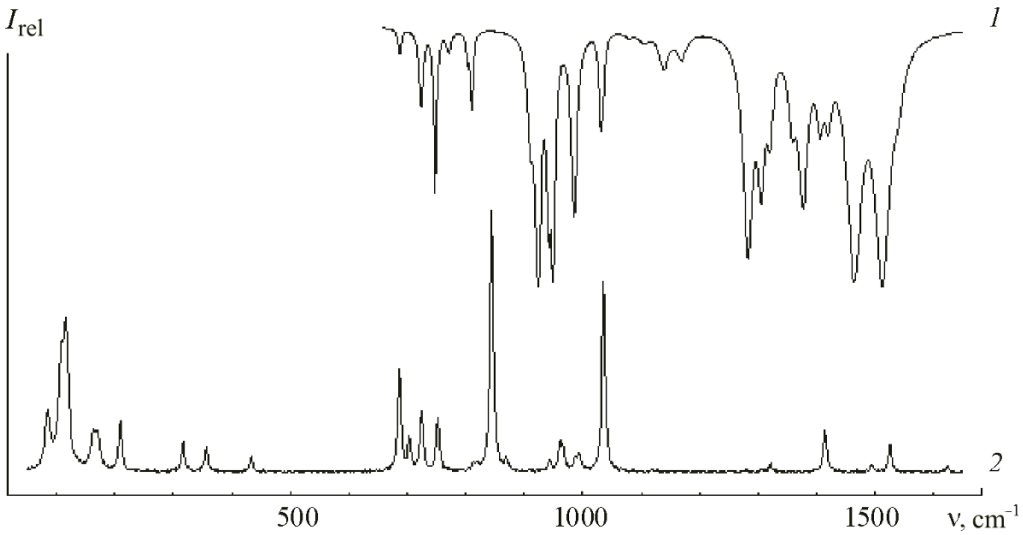

Fig. 1. IR (1) and Raman (2) spectra of $UO_2(NO_3)_2 \cdot 2DMSO$.

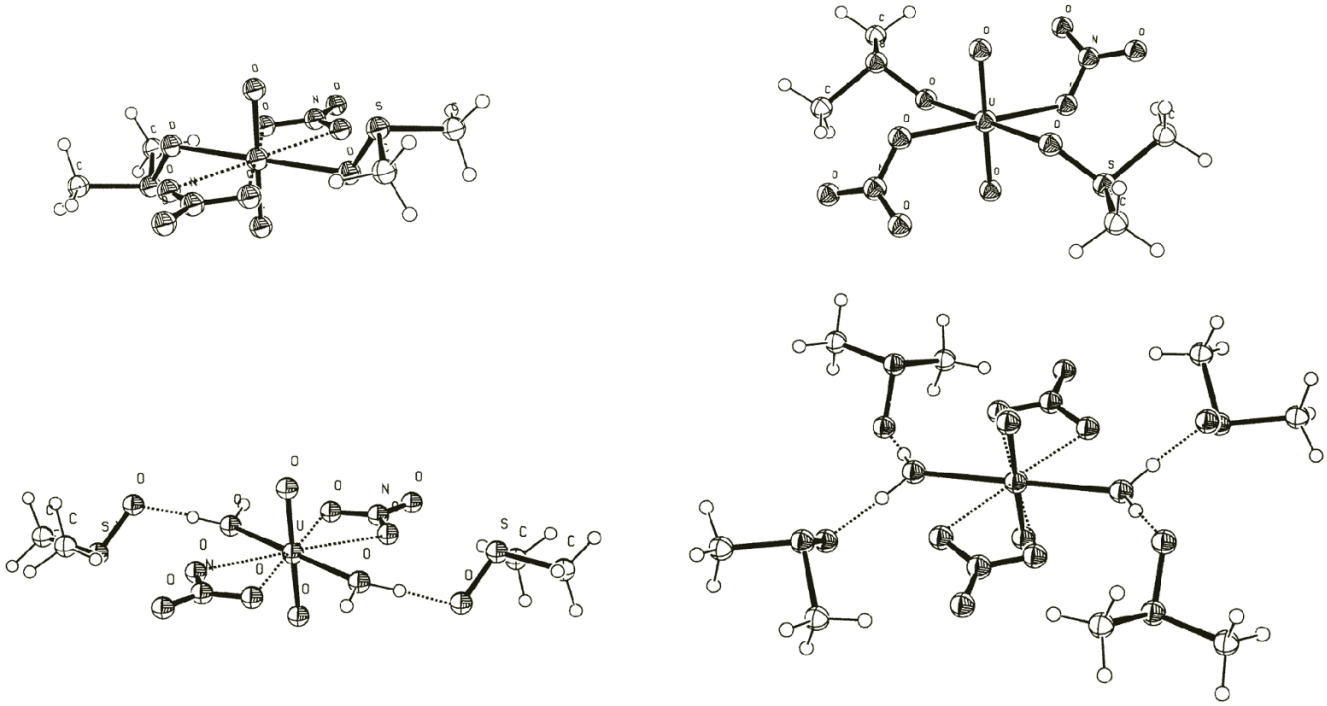

Fig. 2. Equilibrium structures of complexes with bidentate and monodentate nitrate $[UO_2(NO_3)_2 \cdot 2DMSO]$ (a, b); $UO_2(NO_3)_2 \cdot 2H_2O \cdot 2DMSO$ (c); and $UO_2(NO_3)_2 \cdot 2H_2O \cdot 4DMSO$ (d).

the IR spectrum at ~3440, 3193, 2725, 2673, 2545, 1079, and 724 cm^{-1} and strong ones at 2953, 2924, 2870, 2853, 1465, 1377, 1305, and 1170 cm^{-1} belonged to the solvent (mineral oil). Therefore, they are not included in Table 1. Furthermore, broad bands and weak lines in the short-wavelength region (3370–3300 cm^{-1}) were consistent with traces of H_2O in the sample. This allowed the asymmetric shoulder of the strong band at 1513 cm^{-1} to be interpreted as a H_2O bending vibration; the weak line at ~356 cm^{-1}, a H_2O librational vibration.

TABLE 1. Calculated and Experimental Vibrational Frequencies (ν, cm^{-1}) of $UO_2(NO_3)_2 \cdot 2DMSO$ (I), $UO_2(NO_3)_2$ (II), $UO_2(NO_3)_2 \cdot 2H_2O$ (III), $UO_2(NO_3)_2 \cdot 2H_2O \cdot 2DMSO$ (IV), and $UO_2(NO_3)_2 \cdot 2H_2O \cdot 4DMSO$ (**V**) and Their Fragments

Assignment	I				Fragments: UO_2^{2+}, NO_3^-, or DMSO		II		III		IV	V
	ν_{exp}		ν_{calc}		ν_{exp}	ν_{calc}	ν_{exp}	ν_{calc}	ν_{exp}	ν_{calc}	ν_{calc}	ν_{calc}
	IR	Raman scattering	BC	MC								
$\nu_{as}(CH_3)$			3183	3185		3154					3180	3213
$\nu_{as}(CH_3)$			3182	3178		3143					3169	3168
$\nu_{as}(CH_3)$	3013	3019	3175	3164		3137					3145	3151
$\nu_{as}(CH_3)$			3162	3148	2999 [21]	3131					3140	3123
$\nu_s(CH_3)$		2928	3054	3054		3030					3035	3043
$\nu_s(CH_3)$			3052	3034	2915 [21]	3024					3030	3000
Overtone 1406		2803										
ν_s(NO) BC ($\nu_3(NO_3^-)$)		1526	1623	1627	1390 [1]	1381	1635 [22]	1676	1605 [5]	1666	1622	1594
ν_{as}(NO) BC ($\nu_3(NO_3^-)$)	1513		1614	1630			1616 [22]	1663		1654	1612	1584
Overtone 748		1495										
$\delta_{as}(CH_3)$			1456	1466	1438 [21]	1449					1460	1459
$\delta_{as}(CH_3)$	1421	1420	1432	1434		1429					1435	1445
$\delta_{as}(CH_3)$		1415	1422	1427	1414 [23]	1428					1422	1430
$\delta_{as}(CH_3)$	1406		1408	1412	1407 [21]	1413					1410	1421
ν_s(NO) ($\nu_3(NO_3^-)$)			1328	1346			1235 [22]	1249	1280 [5]	1290	1340	1327
ν_{as}(NO) MC ($\nu_3(NO_3^-)$)	1321	1322		1331	1390 [1]	1381						
ν_{as}(NO) BC ($\nu_3(NO_3^-)$)	1283	1280	1316				1220 [22]	1236	1280 [5]	1281	1333	1323
$\delta_s(CH_3)$		1310	1327	1339	1313 [21]	1325					1313	1321
$\delta_s(CH_3)$			1312	1337							1312	1295
$\delta_s(CH_3)$			1301	1308	1290 [23]	1299					1290	1314
$\delta_s(CH_3)+\delta(NO_3)$			1295	1307							1289	1310
C. 705 + 434	1140											
C. 950 + 170		1120										
ν_s(NO) BC ($\nu_1(NO_3^-)$)		1036	1064	1012	1050 [1]	1054	1010 [22]	1041	1027 [5]	1061	1071	1059
ν_{as}(NO) BC ($\nu_1(NO_3^-)$)	1035		1063	995						1056	1071	1057
$\rho(CH_3)$	1030		1039	1042	954 [21]	1007					1025	1032
C. 911+85		995										
$\rho(CH_3)$	986	988	996	990	920 [21]	926					944	947
C. 803+163		967										
C. 845+117		961										
ν_{as}(UO) BC ($\nu_3(UO_3^{2+})$)	950		952		1020–800 [1, 24]	1090	990–965 [22]	976	929 [5]	962	964	958
ν_{as}(UO) MC ($\nu_3(UO_3^{2+})$)	942	944		947								
ν(S=O) BC	924		948 939		1039 [21]	1086					991 991	1004 997
ν(S=O) MC	911			928 919								

TABLE 1 (continued)

Assignment	I				Fragments: UO_3^{2+}, NO_3^-, or DMSO		II		III		IV	V
	ν_{exp}		ν_{calc}		ν_{exp}	ν_{calc}	ν_{exp}	ν_{calc}	ν_{exp}	ν_{calc}	ν_{calc}	ν_{calc}
	IR	Raman scattering	BC	MK								
$\rho(CH_3)$			937	942	900 [21]	892					931	925
$\rho(CH_3)$	870	870	909	915		868					896	902
C. 686+163		850										
$\nu_s(UO)$ ($\nu_1(UO_3^{2+})$)		845	861	855	900–780 [1, 24]	993	895 [22]	885	855 [25]	872	875	872
$\rho(NO_3)$ ($\nu_2(NO_3^-)$)	811	814	819	813	830 [1]	995	798 [22]	807	803 [5]	810	815	814
C. 687+117	803											
C. 687+85	771											
$\delta_s(NO_3)$ BC ($\nu_4(NO_3^-)$)	748	753	755		720 [1]	734	722 [22]	756	748 [5]	747	763	748
$\delta_s(NO_3)$ MC ($\nu_4(NO_3^-)$)		725		731								
$\delta_{as}(NO_3)$ BC ($\nu_4(NO_3^-)$)	705	704	708				689 [22]	709	748 [5]	715	711	727
$\delta_{as}(NO_3)$ MC ($\nu_4(NO_3^-)$)				686								
$\nu_{as}(CS)$	687	687	687	692	698 [21]	649					674	664
$\nu_s(CS)$			649	653	665 [21]	626					641	639
$\gamma(S=O)$		434	412	415	378 [23]	368					436	424, 389
$\rho(S=O)$		317	345	328	329 [23]	310					339	355, 335
$\delta(OUO) + \delta(CSC)$			300	300								
$\delta(CSC)$			291	297	305 [23]	284					295	299
$\delta(OUO)$ ($\nu_2(UO_3^{2+})$)			284	259	290–240 [1, 22]	259	265–250 [22]		196 [25]		268	278
			277	248				319			255	261
$\tau(CH_3)$			270	285		188					243	247
Libration UO_2			216	205				249		271	200	215
$\nu(U\ldots O)$ (nitrate)		209	214	316			252 [25]		264 [25]	252	246	254
			209							284	240	252
			208	303					256 [25]	246	234	224
			199							229	221	223
Libration NO_3			190								203	194
Libration DMSO + $\delta(NO_3^-)$		171	182								158	172
			164							276	157	130
		163	159								128	128
			155					157		157	112	123
Phonon lines		117										
		108										
		85										

Note. The presence of two (or four) identical fragments (NO_3^-, H_2O, or DMSO) in the complexes doubled the frequencies, the splitting of which was as a rule <3 cm^{-1}. Therefore, only one (the greater) wavenumber is given. C. is a combination frequency; BC, bidentate coordination; MC, monodentate coordination; ν, stretching; δ, bending; ρ, rocking; γ, out-of-plane; τ, torsion; s, symmetric; as, antisymmetric vibrations.

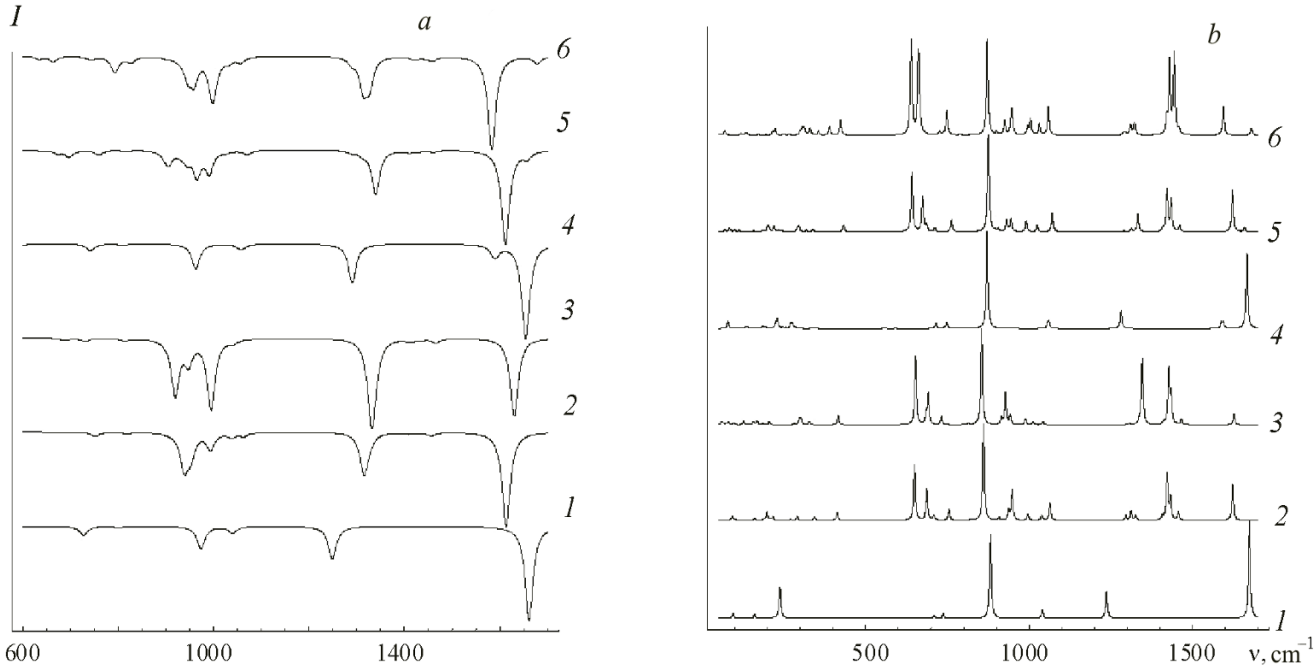

Fig. 3. Calculated IR (a) and Raman (b) spectra of $UO_2(NO_3)_2$ (1); $UO_2(NO_3)_2 \cdot 2DMSO$ (bidentate and monodentate coordination) (2, 3); $UO_2(NO_3)_2 \cdot 2H_2O$ (4); $UO_2(NO_3)_2 \cdot 2H_2O \cdot 2DMSO$ (5); and $UO_2(NO_3)_2 \cdot 2H_2O \cdot 4DMSO$ (6).

The starting model of the $UO_2(NO_3)_2 \cdot 2DMSO$ structure was based on bidentate nitrate coordination in the equatorial plane of the uranyl, which was a more stable configuration than the monodentate form [1]. The model equilibrium structure for bidentate coordinated $UO_2(NO_3)_2 \cdot 2DMSO$ had C_i symmetry. Its structure was analogous to those of $UO_2(NO_3)_2$ complexes with two DMF, dibutylformamide, and dicyclohexylformamide molecules [5]. The organic ligands were located in *trans*-positions relative to the central U atom with the oxygen atoms of the organic ligands situated in the uranyl equatorial plane. Spectra of $UO_2(NO_3)_2 \cdot 2DMSO$ in the region <1000 cm^{-1} showed an anomalously large number of bands and lines that could not be adequately interpreted based only on bidentate NO_3^- coordination. Therefore, we also examined the version with monodentate nitrate coordinated to uranyl. Because the computations indicated that the energy of monodentate coordinated $UO_2(NO_3)_2 \cdot 2DMSO$ was ~51 kJ/mol greater than that of the bidentate complex, it was assumed that the intensities of the corresponding bands and lines of the first complex would be significantly less than those of the second. The equilibrium configurations were found (Fig. 2) and vibrational spectra (Fig. 3) of the separate fragments [UO_3^{2+}, NO_3^-, DMSO, H_2O, $UO_2(NO_3)_2$] were calculated for a comprehensive analysis of the spectral characteristics of the examined systems and for a determination of the spectral and structural features upon hydration of the complexes in the aforementioned approximation. The proposed structural models (Fig. 2) were based on an analysis of the ability to accommodate H_2O and DMSO in the first (inner) coordination sphere of uranyl. Two factors could play the main role. These were the displacing power of the ligand (donor number D) and steric issues. Although the first factor for organics was greater than for H_2O (D_{DMSO} = 29, D_{H_2O} = 14), the larger size of DMSO did not allow it to replace H_2O. Therefore, DMSO could be expelled into the outer coordination sphere of $UO_2(NO_3)_2$.

Structural and spectral characteristics of the isolated uranyl ion and DMSO molecule in the B3LYP/cc-pVDZ approximation and their agreement with experimental data were discussed by us previously [6, 7]. The standard designations ν_1, totally symmetric stretching; ν_2, doubly degenerate bending; and ν_3, asymmetric stretching vibration were used to classify vibrations of the UO_2^{2+} fragment ($D_{\infty h}$ symmetry).

The structure and vibrational spectrum of NO_3^- were calculated for a model with point symmetry D_{3h} (free nitrate). The standard designations ν_1, totally symmetric stretching, ν_2; out-of-plane bending; ν_3, doubly degenerate stretching; and ν_4, doubly degenerate in-plane bending vibration were used to classify vibrations of the NO_3^- fragment.

Two models were also examined for the structure of isolated $UO_2(NO_3)_2$, i.e., bidentate and monodentate nitrates. In the first instance, an equilibrium geometry with D_{2h} symmetry was obtained. The lack of imaginary frequencies in the calculated spectrum confirmed that this configuration was stable. Neither of the models with symmetry limitations (D_{2h}, C_i, etc.) produced an equilibrium configuration for monodentate coordination (calculated vibrational spectra of all models contained several imaginary frequencies). Optimization of the geometry of $UO_2(NO_3)_2$ with monodentate nitrates without symmetry limitations produced an equilibrium configuration with bidentate coordination. Thus, we supposed that free $UO_2(NO_3)_2$ with monodentate coordination was unstable. This structure could be stabilized either by coordination of additional ligands in the first coordination sphere of $UO_2(NO_3)_2$ or in a crystalline sample [22].

The calculated vibrational frequencies (taking into account typical errors of the used approximation), their sequences, and activities in IR and Raman spectra of isolated nitrate and bidentate nitrate coordinated to $UO_2(NO_3)_2$ corresponded to the published values [1, 22, 26] (Table 1). The local symmetry of the nitrate fragment was reduced to C_{2v} for both bidentate and monodentate coordination. As a result, the doubly degenerate modes were split (for typical values, see the literature [1]). The presence of two nitrates in the complex (regardless of their coordination) caused additional splitting of each vibrational mode into two components that were symmetric and asymmetric relative to the complex center. The sizes of these splittings could differ substantially for bi- and monodentate coordinated nitrate (Table 1). This allowed vibrational spectra of $UO_2(NO_3)_2 \cdot 2DMSO$ to be interpreted as follows.

Methyl stretching and bending vibrations are usually found in the ranges 2970–2870 and 1450–1370 cm^{-1} [27]. The CH_3 asymmetric stretching vibration in DMSO exceeded the indicated upper limit of the corresponding range [7, 21, 28]. This allowed strong lines at 3019 and 2928 cm^{-1} in the Raman spectrum to be assigned to asymmetric and symmetric CH_3 stretching vibrations and a weak line at 2803 cm^{-1} to be interpreted as an overtone of a CH_3 bending vibration (1406 cm^{-1}). The weak line at 1495 cm^{-1} lay significantly higher than typical $\delta(CH_3)$ values and was most likely an overtone of bending mode $\nu_4(NO_3^-)$ (bidentate coordination), the main frequency of which appeared as a strong band at ~748 cm^{-1} in the IR spectrum, and a weak line at ~753 cm^{-1} in the Raman spectrum. Bands and lines at 1421 (IR and Raman), 1415 (Raman), 1406 (IR), and 1310 cm^{-1} (Raman) were assigned to methyl bending vibrations based on calculations and the literature [7, 21, 28]. Bands and lines at 1030 (IR), 988 (Raman), 986 (IR), and 870 cm^{-1} (Raman and IR, shoulder) were assigned to rocking vibrations $\rho(CH_3)$ [7, 21, 28].

Calculations predicted a significant (164 cm^{-1}) long-wavelength shift for the S=O stretching frequency in $UCl_4 \cdot 2DMSO$ [7]. This was confirmed in the experimental spectrum of $UCl_4 \cdot 2DMSO$ [21] because $\nu_{S=O}$ was shifted from 1039 cm^{-1} for pure DMSO to 940 cm^{-1} in the complex. Thus, it could be assumed that the quantum-chemical calculation using B3LYP/cc-pVDZ elevated $\nu_{S=O}$ in the complex by ~20 cm^{-1}. It could be proposed that these frequencies in the spectrum were located at ~920 cm^{-1} because an analogous calculation for $UO_2(NO_3)_2 \cdot 2DMSO$ with bidentate nitrates predicted for $\nu_{S=O}$ values of 948 (symmetric mode) and 939 cm^{-1} (asymmetric). Thus, the strong band at 924 cm^{-1} and the shoulder at 911 cm^{-1} in the IR spectrum of $UO_2(NO_3)_2 \cdot 2DMSO$ were assigned to S=O stretching vibrations for bi- and monodentate nitrates, respectively.

Frequencies of C–S stretching vibrations in pure DMSO are located at 695 (asymmetric mode) and 665 cm^{-1} (symmetric) [21, 28]. The first of these frequencies was shifted to 786 cm^{-1} for $UCl_4 \cdot 2DMSO$ [7, 21]. One of the four possible C–S stretching modes (asymmetric relative to the S atom and symmetric relative to the U atom according to calculations) in the studied complex corresponded to a medium line at 687 cm^{-1} in the Raman spectrum. The corresponding band (asymmetric vibration relative to the S atom and U atom according to calculations) in the IR spectrum was very weak. Weak lines at 434 and 317 cm^{-1} in the Raman spectrum were assigned to out-of-plane bending γ and rocking ρ S=O vibrations (bands at 424 and 315 cm^{-1} in the spectrum of $UCl_4 \cdot 2DMSO$ corresponded to these vibrations [7, 21]).

Strong bands at 950 (bidentate coordination) and 942 cm^{-1} (monodentate) in the IR spectrum were assigned to the asymmetric ν_3 uranyl stretching vibration; the strong line at 845cm^{-1} in the Raman spectrum, to totally symmetric ν_1. Bands and lines for uranyl ν_2 bending mode were reported in the range 290–240 cm^{-1} depending on the type of coordination and number and type of ligands [1, 22, 29]. The ν_2 vibration was assigned to a lower-frequency region (210–190 cm^{-1}) [24, 25]. According to our calculations, which reproduced highly successfully the structure, and frequencies and intensities of uranyl stretching modes, the frequency of the ν_2 vibration was 259 cm^{-1} and; therefore, fell into the first of the mentioned ranges. The calculated intensity of this mode was low. We supposed that this line was not observed in the Raman spectrum of the studied complex.

The doubly degenerate ν_3 stretching vibration of complexed nitrate was split into high-frequency (symmetric component observed at 1526 cm^{-1} in the Raman spectrum; asymmetric, 1513 cm^{-1} in the IR spectrum) and low-frequency

(~1280 cm^{-1} in IR and Raman) modes [1]. Other nitrate vibrational frequencies appeared near 1035 (IR and Raman, ν_1), 811 (IR, out-of-plane ν_2), 750 (IR and Raman, symmetric component of ν_4), and 705 cm^{-1} (IR and Raman, asymmetric component of ν_4). The calculated and experimental data [1, 22, 26] also agreed.

Frequencies of coordinated U…O stretching vibrations were reported at ~200 cm^{-1} for bidentate nitrate coordination. This allowed a weak line at 209 cm^{-1} in the Raman spectrum to be assigned to $\nu_{U...O}$ (the mode at 199 cm^{-1} was the strongest of the four vibrations of this type predicted by the calculations). Two weak lines at 171 and 163 cm^{-1} corresponded according to the calculations to ligand (DMSO) bending vibrations relative to uranyl. The lower-frequency region contained according to the calculations numerous complicated mixed bending modes of the ligands and uranyl. The frequencies and shapes of these vibrations had little information value and are not given in Table 1. Two medium lines (117 and 108 cm^{-1}) and a weak line at ~85 cm^{-1} in the Raman spectrum were assigned to crystal-lattice vibrations.

Hydration of $UO_2(NO_3)_2$ decreased the high-frequency component of the $\nu_3(NO_3^-)$ vibration to 1635 and 1616 cm^{-1} for $UO_2(NO_3)_2$ [22] and 1605 cm^{-1} for $UO_2(NO_3)_2 \cdot 2H_2O$ [5]. This trend was predicted by our calculations [1676 and 1663 cm^{-1} for $UO_2(NO_3)_2$; 1666 and 1654 cm^{-1} for $UO_2(NO_3)_2 \cdot 2H_2O$; 1622 and 1612 cm^{-1} for $UO_2(NO_3)_2 \cdot 2H_2O \cdot 2DMSO$; and 1594 and 1584 cm^{-1} for $UO_2(NO_3)_2 \cdot 2H_2O \cdot 4DMSO$]. Conversely, the frequency tended to increase for the low-frequency component of this vibration {1235 and 1220 cm^{-1} for $UO_2(NO_3)_2$ [22] and 1280 cm^{-1} for $UO_2(NO_3)_2 \cdot 2H_2O$ [5]}, which in general was confirmed by theoretical calculations [1249 and 1236 cm^{-1} for $UO_2(NO_3)_2$; 1290 and 1281 cm^{-1} for $UO_2(NO_3)_2 \cdot 2H_2O$; 1340 and 1333 cm^{-1} for $UO_2(NO_3)_2 \cdot 2H_2O \cdot 2DMSO$; 1327 and 1323 cm^{-1} for $UO_2(NO_3)_2 \cdot 2H_2O \cdot 4DMSO$]. The situation was analogous for $\nu_1(NO_3^-)$ and $\nu_2(NO_3^-)$ {1010 and 798 cm^{-1} for $UO_2(NO_3)_2$ [22]; 1027 and 803 cm^{-1} for $UO_2(NO_3)_2 \cdot 2H_2O$ [5] (experimental); 1041 and 807 cm^{-1} for $UO_2(NO_3)_2$; 1061 and 810 cm^{-1} for $UO_2(NO_3)_2 \cdot 2H_2O$; 1071 and 815 cm^{-1} for $UO_2(NO_3)_2 \cdot 2H_2O \cdot 2DMSO$; 1059 and 814 cm^{-1} for $UO_2(NO_3)_2 \cdot 2H_2O \cdot 4DMSO$ (calculated)}. Consistent tendencies were not observed for the $\nu_4(NO_3^-)$ mode (Table 1).

Hydration of $UO_2(NO_3)_2$ caused frequencies to decrease for asymmetric $\nu_3(UO_3^{2+})$ and symmetric $\nu_1(UO_3^{2+})$ uranyl stretching vibrations {~980 and 895 cm^{-1} for $UO_2(NO_3)_2$ [22] and 929 and 855 cm^{-1} for $UO_2(NO_3)_2 \cdot 2H_2O$ [5] (experimental); 976 and 885 cm^{-1} for $UO_2(NO_3)_2$; and 962 and 872 cm^{-1} for $UO_2(NO_3)_2 \cdot 2H_2O$ (calculated)}. Insertion of additional ligands into the second coordination sphere had practically no effect on these frequencies (Table 1).

Conclusions. Quantum-chemical modeling of the structure of a $UO_2(NO_3)_2$ complex with two DMSO molecules as electron-donating organic ligands predicted the existence of two stable configurations of C_i symmetry with bidentate and monodentate nitrate coordination to the central U atom. Vibrational IR and Raman spectra of the complex could be interpreted sufficiently completely only by assuming that both coordination types were present. Formation of the complexes was accompanied by splitting of bands and lines of nitrate vibrations and their shifts to short and long wavelengths that were predicted adequately by the calculations. The observed spectral shifts of the S=O and nitrate vibrational frequencies could be used for analytical purposes.

REFERENCES

1. L. V. Volod′ko, A. I. Komyak, and D. S. Umreiko, *Uranyl Compounds* [in Russian], Vol. 1, BGU, Minsk (1981).
2. C. Clavaguera-Sarrio, S. Hoyau, N. Ismail, and C. J. Marsden, *J. Phys. Chem. A*, **107**, 4515–4525 (2003).
3. R. G. Denning, *J. Phys. Chem. A*, **111**, 4125–4143 (2007).
4. L. R. Morss, N. M. Edelstein, and J. Fuger (Eds.), *The Chemistry of the Actinide and Transactinide Elements*, 3rd edn., Springer, Dordrecht [London] (2006).
5. A. Prestianni, L. Joubert, A. Chagnes, G. Cote, M.-N. Ohnet, C. Rabbe, M.-C. Charbonnel, and C. Adamo, *J. Phys. Chem. A*, **114**, 10878–10884 (2010).
6. D. S. Umreiko, M. B. Shundalov, A. P. Zazhogin, and A. I. Komyak, *Zh. Prikl. Spektrosk.*, **77**, No. 4, 550–555 (2010).
7. M. B. Shundalov, P. C. Chibirai, A. I. Komyak, A. P. Zazhogin, and D. S. Umreiko, *Zh. Prikl. Spektrosk.*, **79**, No. 2, 181–188 (2012).
8. M. B. Shundalau, A. I. Komiak, A. P. Zajogin, and D. S. Umreiko, *J. Spectrosc. Dyn.*, **3**, 4 (2013).
9. M. W. Schmidt, K. K. Baldrige, J. A. Boatz, S. T. Elbert, M. S. Gordon, J. H. Jensen, S. Koseki, N. Matsunaga, K. A. Nguyen, S. J. Su, T. L. Windus, M. Dupuis, and J. A. Montgomery, *J. Comput. Chem.*, **14**, 1347–1363 (1993).
10. http://www.msg.ameslab.gov/GAMESS/GAMESS.html
11. B. M. Bode and M. S. Gordon, *J. Mol. Graphics Modell.*, **16**, 133–138 (1998).
12. L. J. Farrugia, *J. Appl. Crystallogr.*, **30**, 565 (1997).

13. L. R. Kahn, P. J. Hay, and R. D. Cowan, *J. Chem. Phys.*, **68**, 2386–2397 (1978).
14. T. H. Dunning, Jr., *J. Chem. Phys.*, **90**, 1007–1023 (1989).
15. https://bse.pnl.gov/bse/portal
16. D. Feller, *J. Comput. Chem.*, **17**, 1571–1586 (1996).
17. K. L. Schuchardt, B. T. Didier, T. Elsethagen, L. Sun, V. Gurumoorthi, J. Chase, J. Li, and T. L. Windus, *J. Chem. Inf. Model.*, **47**, 1045–1052 (2007).
18. A. D. Becke, *J. Chem. Phys.*, **98**, 5648–5652 (1993).
19. C. Lee, W. Yang, and R. G. Parr, *Phys. Rev. B: Condens. Matter Mater. Phys.*, **37**, 785–789 (1988).
20. P. J. Stephens, F. J. Devlin, C. F. Chabalowski, and M. J. Frisch, *J. Phys. Chem.*, **98**, 11623–11627 (1994).
21. A. P. Zazhogin, A. I. Komyak, and D. S. Umreiko, *Zh. Prikl. Spektrosk.*, **75**, No. 5, 729–732 (2008).
22. L. V. Kobets, G. N. Klavsut′, and D. S. Umreiko, *Zh. Neorg. Khim.*, **26**, 173–178 (1981).
23. M. Tranquille and M. T. Forel, *Spectrochim. Acta, Part A*, **28**, 1305–1320 (1972).
24. W. A. de Jong, R. J. Harrison, J. A. Nichols, and D. A. Dixon, *Theor. Chem. Acc.*, **107**, 22–26 (2001).
25. J. R. Ferraro and A. Walker, *J. Chem. Phys.*, **45**, 550–553 (1966).
26. M. Tsuboi and I. C. Hisatsune, *J. Chem. Phys.*, **57**, 2087–2093 (1972).
27. R. M. Silverstein, F. X. Webster, and D. J. Kiemle, *Spectrometric Identification of Organic Compounds*, John Wiley & Sons, Hoboken, NJ (2005).
28. F. A. Cotton, R. Francis, and W. D. Horrocks, Jr., *J. Phys. Chem.*, **64**, 1534–1536 (1960).
29. H. D. Bist, *J. Mol. Spectrosc.*, **27**, 542–544 (1968).